Proceedings of the ASME 2016 Dynamic Systems and Control Conference
DSCC2016
October 12-14, 2016, Minneapolis, Minnesota, USA

DSCC2016-9802

STATE OF CHARGE ESTIMATION FOR AN ELECTRIC WHEELCHAIR USING A FUEL GAUGE MODEL

Christopher Miller[†] **Kelilah Wolkowicz**[‡] **Jariullah Safi**[‡] **Sean N. Brennan**[‡*]

[†]Department of Electrical Engineering
The Pennsylvania State University
University Park, PA

[‡]Department of Mechanical and Nuclear Engineering
The Pennsylvania State University
University Park, PA

ABSTRACT

Electric wheelchair users depend on a reliable power system in order to regain mobility in their daily lives. If a wheelchair's battery power depletes without the user being aware, the individual may become stranded, further limiting their freedom of mobility and potentially placing the user in a harmful situation. This research seeks to develop a State-of-Charge (SOC) estimator for the batteries of an electric wheelchair. A second-order equivalent circuit battery model is developed and parameterized for a wheelchair's lead-acid battery pack. To simplify the SOC estimation, this algorithm models a vehicle's fuel gauge. A coulomb accumulator is incorporated to estimate energy usage in the non-linear region of the OCV-SOC curve, while a Kalman filter is used to estimate SOC in the linear region of the curve. The estimator is verified using experimentally collected data on-board a robotic wheelchair. The implementation of these algorithms with powered wheelchairs can significantly improve the estimation of wheelchair battery power and can ultimately be coupled with warning systems to alert users of depleting battery life, as well as enable low-power modes to increase wheelchair user safety.

1 INTRODUCTION

Significant research has been conducted in the area of intelligent electric wheelchairs since the 1980s [1]. Notably absent from the literature is a large body of research aimed at power wheelchair energy estimation and electric range. Exceptions include the research conducted by Cooper, *et al.*, to determine the driving habits of electric wheelchair users. Their research showed that average powered-wheelchair users may travel less than eight km per day [2]. However, this work did not include information regarding the electric range or number of recharges for a given day; only estimates based upon a user's daily driving habits were presented. In a follow-up paper, Cooper, *et al.* estimates the electric range of multiple wheelchairs; however, no general consensus is presented and as the ranges vary from 23.6 km to 57.7 km [3].

There has also been some investigation into methods to estimate energy usage of assistive technologies, the most widely cited of which may arguably be the work of Aylor, *et al.*. Aylor, *et al.* designed a simple approach to estimate the State-of-Charge (SOC) of a battery by measuring the open circuit voltage (OCV) of a wheelchair's battery [4]. At the time the work was the published in the early 1990s, their estimator yielded results comparable to industrial battery fuel gauges for level surfaces. However, on sloped surfaces this technique lost some of its initially determined accuracy. The methods developed by Aylor, *et al.*, are presently the most widely cited methods in electric wheelchair battery SOC estimation and are very feasible for implementation on an electric wheelchair.

Since the 1990s, others have established different means of estimating wheelchair energy usage. For example, Chen, *et al.*, developed a system to estimate the remaining SOC and electric range on a wheelchair battery using fuzzy logic and neural networks [5]. Their results indicated that these methods are feasi-

*Address all correspondence to sbrennan@psu.edu.

ble on electric wheelchairs; however, these methods are atypical in the area of battery research, which typically prefer a model-based approach for energy estimation. Further, Chen, *et al.*, used a lithium ion battery as their energy source, whereas most wheelchairs use lead acid batteries.

In recent years, additional methods of extending battery capacity in wheelchairs have been presented. Bouquain, *et al.*, demonstrated a method to extend the range of an electric wheelchair by using a hydrogen fuel cell and a DC-to-DC converter to provide constant power to a wheelchair with slowly changing dynamics (e.g. constant velocity, straight line motion) [6]. As the dynamics increase (e.g. sudden turns), a lead acid battery will source power to the wheelchair while the fuel cell builds up the desired power. Yang, *et al.*, presented a different hybrid hydrogen fuel cell and battery wheelchair power supply [7]. The authors proposed a system where a primary battery is sourcing power to the wheelchair's drive-train while a secondary battery is either idling or being recharged by the hydrogen fuel cell. When the primary battery's voltage decreases below a particular cutoff voltage, the battery packs switch roles, such that the secondary battery sources current to the drive-train while the primary battery pack is recharged by the hydrogen fuel cell. Some of the methods presented in the aforementioned works are not commonly used in battery estimation and may prove to be difficult to implement on commercially available electric wheelchairs.

The purpose of this paper is to expand upon and modernize existing wheelchair energy estimation research and improve the safety of electric wheelchair operation by providing users with a more accurate estimate of the state of charge remaining on their battery pack. First, Section 2 describes the model developed to estimate the battery's State-of-Charge. In Section 3, the methods used to identify the battery pack's parameters are presented. Section 4 presents the robotic wheelchair platform and discusses experimental design. Next, Section 5 discusses the results obtained. Finally, in Section 6, the contributions of this work and future work are discussed.

2 METHODOLOGY

This section will provide an overview of the methods used to estimate the wheelchair's battery pack's SOC. First, the fuel gauge model will be presented. Then, the battery's equivalent circuit model will be discussed. Finally, the coulomb counter and Kalman filter used by the fuel model for SOC estimation will be described

2.1 The Fuel Gauge Model

Consider the functionality of an automotive fuel gauge. A vehicle's fuel gauge remains at full for a long time after the tank has been filled with gasoline. This phenomenon occurs to compensate for the non-linearities that are present when measuring

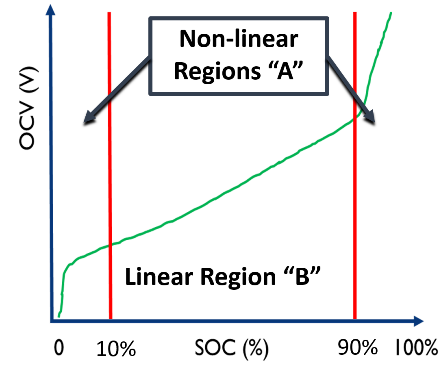

FIGURE 1: In the fuel gauge model, coulomb counting will be implemented in the non-linear regions for SOC estimation, while a Kalman filter will be used in the linear region.

fluid volume in a full container, as discussed in [8]. After a given threshold is reached, the fuel measurements begin to decrease with a direct relation to remaining fuel volume. Lastly, once a second threshold is reached, the fuel gauge will display empty even if some fuel remains in the fuel tank. This phenomenon occurs to account for consumers who prefer to drive their vehicle with little fuel remaining and to account for the non-linearities associated with measuring fluid volume when the tank is nearly empty.

The fuel gauge model presented is analogous to the method used in this work to estimate the wheelchair lead acid battery pack's SOC. In the fuel gauge model, a coulomb counter estimates the SOC of the battery pack in the two non-linear regions of the battery pack, defined here as 0% to 10% SOC and 90% to 100% SOC. The idea of estimating SOC in this manner is not novel; Codeca *et al.* presented a similar method piece-wise method [9]. In the linear region of the battery pack, a Kalman filter predicts the SOC using the model presented in Section 2.2. A diagram presenting this method in further detail is depicted in Figure 1. Thus, like an automotive fuel gauge, the proposed wheelchair fuel gauge is intentionally changing estimator behavior in the extreme ends of the curves describing the remaining capacity.

2.2 The Battery Model

A second order equivalent-circuit model was selected to model the wheelchair's battery pack and is illustrated in Fig. 2. The model is based on the work presented by Plett and Coleman, *et al.* [10–12].

Applying Kirchoff's voltage laws to the second-order equivalent circuit battery model, the voltage across the battery pack's terminals can be expressed as

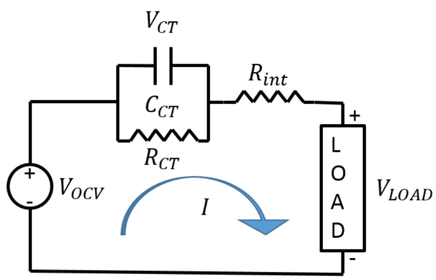

FIGURE 2: The second-order, equivalent-circuit battery model.

$$V_{LOAD} = V_{OCV} - R_{int} I(t) - V_{CT} \tag{1}$$

where $I(t)$ represents the current flowing from the battery pack to the wheelchair system, V_{CT} represents the voltage across the battery's resistor-capacitor (RC) network, and V_{OCV} is a function of the battery's SOC, as shown in the relationships presented by Eqs. (2) and (3):

$$V_{OCV}(SOC) = SOC \cdot \alpha + \mu \tag{2}$$

$$SOC = 1 - \frac{1}{Q_0}\int_{t_0}^{t} I(\tau)d\tau \tag{3}$$

where α is a constant parameter relating SOC to voltage and μ represents the cutoff voltage of the battery pack. The battery cutoff voltage can be found in the battery's data sheet or user-selected to vary model performance. A user may choose a value for μ lower than the manufacturer specification if they would like to further discharge their battery pack or a higher-than-specified value to extend the pack's overall lifetime. A higher order model was not selected in order to maintain model simplicity. Furthermore, some literature indicates that higher and infinite-order models are not only computationally impractical, but yield negligible improvements in SOC estimation [13]. It has also been shown that a second-order model, such as the one presented, is generally sufficient for accurate estimator performance [12].

To practically implement the model presented by Eqs. (1) - (3), these functions are transformed into state space representation. The model's state vector is presented in Eq. (4), the model's inputs are presented in Eq. (5), and the model's output is presented in Eq. (6).

$$x = \begin{pmatrix} V_{CT} \\ SOC \end{pmatrix} \tag{4}$$

$$u(t) = \begin{pmatrix} I(t) \\ \mu \end{pmatrix} \tag{5}$$

$$y(t) = V_{LOAD} \tag{6}$$

The form of the continuous-time state space representation of the model is presented in Eqs. (7) and (8):

$$\dot{x} = Ax + Bu(t) + w, \quad w \sim \mathcal{N}(0,Q) \tag{7}$$

$$y = Cx + Du(t) + v, \quad v \sim \mathcal{N}(0,R) \tag{8}$$

where Q represents the variance associated with the process noise and R represents the variance associated with the measurement noise. The system dynamics are explicitly given in Eqs. (9) and (10):

$$\dot{x} = \begin{pmatrix} -\tau_{CT}^{-1} & 0 \\ 0 & 0 \end{pmatrix} x + \begin{pmatrix} C_{CT}^{-1} & 0 \\ -Q_0^{-1} & 0 \end{pmatrix} u(t) + w \tag{9}$$

$$y(t) = \begin{pmatrix} -1 & \alpha \end{pmatrix} x + \begin{pmatrix} -R_{int} & 1 \end{pmatrix} u(t) + v \tag{10}$$

where τ_{CT} represents the RC time constant, C_{CT} represents the RC pair's capacitance, and R_{int} represents the battery pack's internal resistance.

The system model presented in Eqs. (7) - (10) is descritized using a zero-order hold.

2.3 The Coulomb Counter

To estimate the battery pack's SOC in the non-linear regions of the OCV-SOC curve, a coulomb counter is implemented, as shown in Eq. (3). A coulomb counter is only used to estimate the non-linear regions of the OCV-SOC curve in order to simplify the overall estimation algorithm. This method is not used to estimate SOC for the entirety of the OSC-SOC curve because the accumulator does not account for battery dynamics and it, alone, cannot compensate for model drift as the battery pack ages [11, 14].

2.4 The Kalman Filter

In the linear region of the OCV-SOC curve ($10\% < SOC < 90\%$), a linear Kalman Filter is used to estimate the SOC as described by [15]. The prediction equations are given by Eqs. (11) and (12) and the measurement update equations are given by Eqs. (13) - (16):

$$\hat{x}_{k|k-1} = A\hat{x}_{k-1|k-1} + Bu_{k-1} \tag{11}$$

$$P_{k|k-1} = AP_{k-1|k-1}A^T + Q \tag{12}$$

$$K_k = P_{k|k}C^T(CP_{k|k-1}C^T + R)^{-1} \tag{13}$$

$$\tilde{y}_k = y_k - (C\hat{x}_{k|k-1} + Du(k)) \tag{14}$$

$$\hat{x}_{k|k} = \hat{x}_{k|k-1} + K_k\tilde{y}_k \tag{15}$$

$$P_{k|k} = (I - K_kC)P_{k|k-1} \tag{16}$$

where P represents the covariance matrix and K represents the Kalman gain.

Given the battery model, pack voltage, and current measurements, the Kalman filter is able to predict the SOC estimate and compensate for un-modeled battery dynamics and system noise [11, 16].

3 MODEL IDENTIFICATION

The battery model and estimation scheme have been presented, but their parameters have not yet been identified. The battery's capacity, as well as the parameters α and μ are found from the battery pack's OCV-SOC curve. To find this OCV curve, the battery pack is fully charged and then is discharged at a rate of 1A until the pack's cutoff voltage, as listed in the data sheet, is reached. During the battery's discharge, a DAQ system samples the pack voltage. This procedure is performed three times. The resulting OCV-SOC curves for the lead acid battery pack are presented in Fig. 3. To determine the capacity parameter, Q_0, the constant current for each test is integrated with respect to time over the duration of the complete discharge and the three resulting values are averaged. This value is given in Table 1.

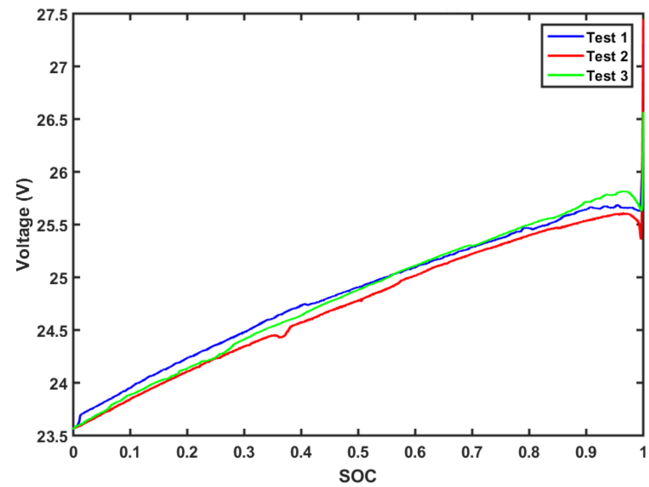

FIGURE 3: The OCV-SOC curve of the lead acid battery pack.

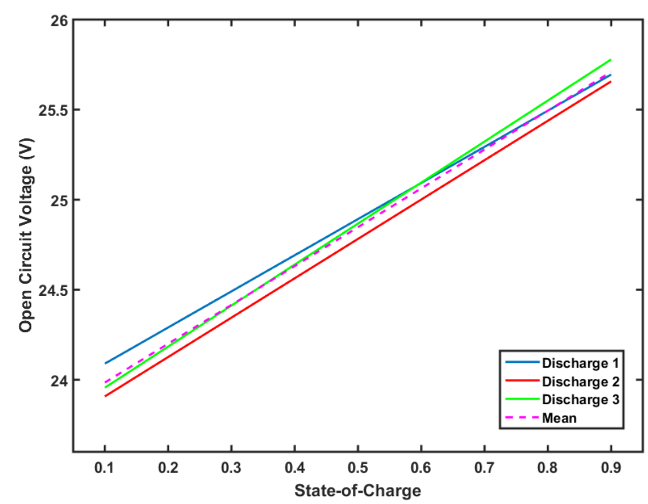

FIGURE 4: The linear regions of the three OCV-SOC discharge tests and the average of the three curves.

To identify the parameters α and μ, a linear regression is performed on the linear region of each OCV-SOC curve. The resulting parameters are then averaged. Fig. 4 presents the linear regions of the OCV-SOC curves and mean curve; Table 1 presents the values for α and μ.

To identify τ_{CT}, R_{int}, C_{CT}, a pulse test is performed. The current profile designed to perform this test is influenced by the US Department of Energy's FreedomCAR Battery Test Manual and the works of Plett and Coleman *et al.* [10, 17, 18]. To perform this pulse test, the battery pack is charged completely and allowed to rest. Then, the battery pack is discharged by 20%

TABLE 1: Battery model parameters derived from the linear region of the OCV-SOC curve.

Parameter	Value
α	2.15 V/SOC
μ	23.77 V
Q_0	1.11E+05 Coulombs

TABLE 2: This table presents the battery model parameters derived from the least squares regression.

Parameter	Value
τ_{CT}	305.77 s
R_{int}	0.108 Ω
C_{CT}	11994 F

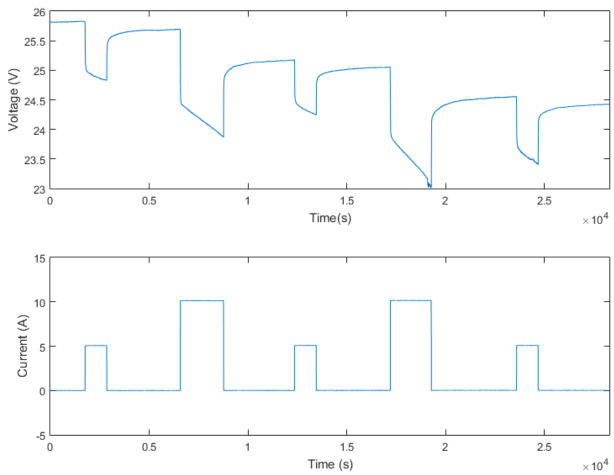

FIGURE 5: The measured voltage (top) and current (bottom) from the current pulse test.

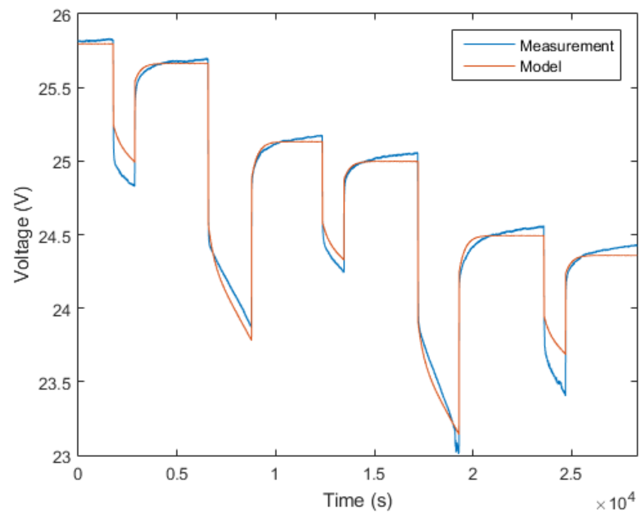

FIGURE 6: This plot presents the fit of the battery model and compares it to the measured battery pack response.

SOC to ensure it has entered the linear region and allowed to rest once more. Next, using a programmable DC load, the battery is discharged using a series of current pulses and the pack voltage is sampled using a custom built DAQ. The DAQ system has a 16-bit resolution and samples the system at 80Hz. The current profile used to discharge the battery pack, as well as the pack's response, is presented in Fig. 5.

Using the response presented in Fig. 5 and the model presented in Eqs. (9) and (10), the parameters τ_{CT}, R_{int}, C_{CT} are identified using least squares regression. The results of this regression are shown in Table 2. A comparison between the model's response and the measured response is presented in Fig. 6.

Finally, the Kalman filter's process covariance matrix, Q, and the sensor's covariance matrix, R are defined. Since the states, SOC and V_{CT} are not correlated, the two-by-two Q matrix is assumed to be diagonal. The states are not correlated because the potential measured across the capacitor is dependent on the load and not the pack's SOC; in other words, the capacitor voltage will not vary uniquely with SOC and vice-versa. The values along the diagonal represent the covariances associated with each state. The covariance for the SOC state is given by the mean error between the values presented in Table 1 and the linear regions of the OCV-SOC curve. The covariance for the V_{CT} state represents the error between the predicted and measured model shown in Fig. 6. The R matrix is a one-by-one matrix defining the voltage sensor's noise characteristics. The values for both the Q and R matrices were further adjusted using experimental data. Table 3 presents the covariances stored in the Q and R matrices.

4 EXPERIMENTATION

This section presents the robotic wheelchair used in testing the estimation algorithm and discusses the methods used to evaluate the estimator's performance

4.1 The Robotic Wheelchair

The robotic wheelchair, shown in Fig. 7, is a modified Jazzy Pride 6 wheelchair by Pride Products Corp, USA. The

TABLE 3: This table presents the Q and R matrix values. The first two terms are associated with the Q matrix and the final term is associated with the R matrix.

Parameter	Value
σ_{SOC}^2	0.0011
$\sigma_{V_{CT}}^2$	3.356
σ_{sens}^2	5.2365

FIGURE 7: The robotic wheelchair.

wheelchair has been retrofitted with a custom power distribution system, a variety of sensors, and an onboard computing system. Of particular importance to this research, is the custom DAQ system able to monitor both the current leaving the battery pack and the voltage across the battery pack. The current measurements are gathered by a LEM CKSR-50-ND current transducer and the voltage measurements are measured via a custom-built voltage sensor. Both are sampled at 80Hz by a 16-bit analog-to-digital converter. The onboard computer reads and saves the data from the DAQ.

4.2 Experimental Design

The wheelchair is first completely charged and allowed to rest. Then, the chair is turned on and the algorithm is initialized; the Kalman Filter's covariance matrix, P, is initialized as Q. During experimentation, a user drives the wheelchair through a pre-planned path consisting of the typical maneuvers an average wheelchair user may perform in an office building. After navigating this path, the wheelchair is parked and again allowed to rest. After rest, the path is traversed once more and this process is repeated until the wheelchair's SOC approaches 0% or until the battery pack voltage falls below the predefined cutoff voltage in order to prevent damage to the battery pack.

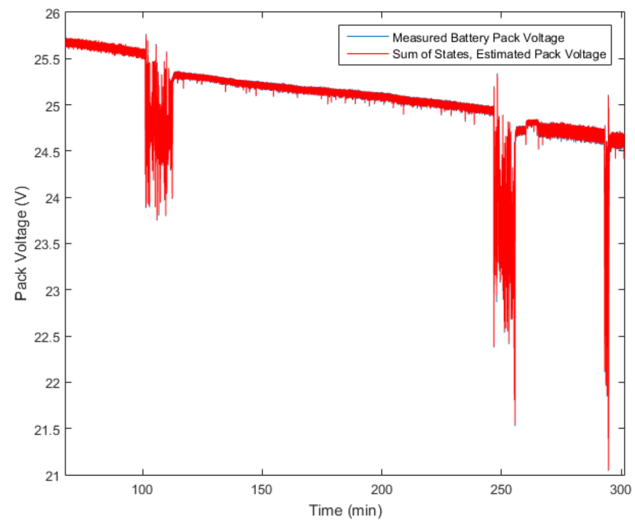

FIGURE 8: This plot presents the sum of the states and compares it to the measured battery pack voltage in the linear region of the OCV-SOC curve.

5 RESULTS

A comparison between the measured and estimated battery pack voltage is shown in Fig. 8. Here, it can be observed that the estimator states track the measured voltage with a mean error of 0.85%. This suggests that the dynamics used in the estimator are fairly representative of the dynamics observed in the states. Similar to the increased slope on the SOC curve, as the battery pack undergoes a larger load, such as when the wheelchair is driven, the battery pack voltage drops. The voltage estimate and measurement for the final driving segment, approximated near 300 minutes, depicts when the cutoff voltage was met and when the test subsequently ended. The test ended when the cutoff voltage was met to prevent damage to the battery pack since operating below the cutoff voltage can cause permanent damage to the battery pack as discussed in the battery's data sheet [19] and in Section 4.2.

The SOC curve obtained during experimentation is presented in Fig. 9. The slope of the SOC curve remains constant at 0.9 SOC when the Coulomb counter stops estimation and the Kalman filter begins. The changes in slope in the SOC curve represent instances where the wheelchair transitions from a resting

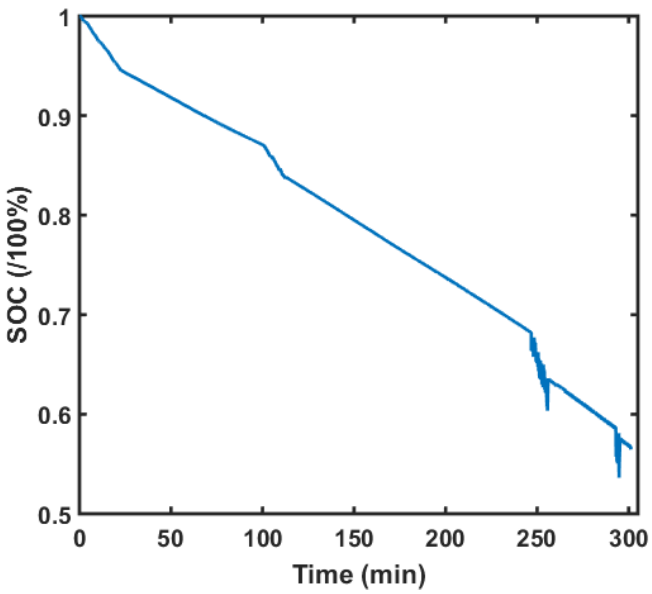

FIGURE 9: Robotic wheelchair SOC estimate.

state to driving state or vice-versa.

True SOC cannot be directly measured using the methods presented, only an estimate of the pack's SOC can be observed. In smaller battery packs that require short durations to rest, the resting open-circuit voltage can be inverted using an OCV-SOC curve after applying a load to find an SOC value for comparison with the estimator's result. However, when using lead acid batteries sized for electric wheelchairs, the resting duration can range from six hours to more than a day, making such an inversion impractical.

The estimated output shown in Fig. 8 sufficiently tracks the measured output, indicating that the modeled dynamics are representative of the battery's dynamics; therefore, the SOC presented in Fig. 9 is an accurate estimate of the pack's SOC. Previous works by the author have shown this model's functionality in simulation [20].

6 CONCLUSIONS AND FUTURE WORK

This research sought to fill a gap in assistive technology literature in the area of energy prediction for electric wheelchairs. This research may be beneficial to both electric wheelchair users and researchers alike. Presently, wheelchair users rely on methods developed in the 1990's to determine when they need to recharge their battery pack. By implementing methods widely used for SOC estimation in the electric vehicle and portable devices industry, electric wheelchair users will be able to better estimate their wheelchair's battery range and make informed decisions about when to recharge their batteries. Improved SOC estimation will not only improve the battery pack life, but will also help to prevent users from becoming stranded and unable to drive to safety as a result of low SOC.

The sum of the states adequately tracked the measured battery pack voltage, thus indicating the estimator accurately models the battery pack's dynamics. Since the estimated states track the output sufficiently, the state dynamics are assumed to be accurate as well and a SOC estimate is found and presented.

Researchers may use this work to develop better SOC estimators for electric wheelchairs or use this work to develop energy-cognizant smart wheelchairs. Furthermore, this research presents another means of estimating lead acid battery pack SOC. While this estimator is implemented on an electric wheelchair, these methods may be used elsewhere.

Smart electric wheelchairs pose a unique opportunity for SOC estimation as they have long idle periods with a small current draw and short periods of large current draw while driving. Developing an SOC estimation algorithm to account for this unique duty cycle may pose an interesting area for expansion in the area of SOC estimation as well. Other possible expansions of this research include implementing estimation of remaining range instead of remaining charge.

ACKNOWLEDGMENT

This material is based upon work supported by the National Science Foundation under Grant No. DGE1255832. Any opinions, findings, and conclusions or recommendations expressed in this material are those of the author(s) and do not necessarily reflect the views of the National Science Foundation.

REFERENCES

[1] Madarasz, R. L., Heiny, L. C., Cromp, R. F., and Mazur, N. M., 1986. "The design of an autonomous vehicle for the disabled". *IEEE Journal of Robotics and Automation,* ***RA-2***(3), September, pp. 117 – 126.

[2] Cooper, R. A., Thorman, T., Cooper, R., Dvorznak, M. J., Fitzgerald, S. G., Ammer, W., Song-Feng, G., and Boninger, M. L., 2002. "Driving characteristics of electric-powered wheelchair users: How far, fast, and often do people drive?". *Archives of Physical Medicine and Rehabilitation,* ***83***(2), pp. 250–255.

[3] Cooper, R. A., VanSickle, D. P., Albright, S. J., Stewart, K. J., Flannery, M., and Robertson, R. N., 1995. "Power wheelchair range testing and energy consumption during fatigue testing". *Journal of rehabilitation research and development,* ***32***(3), pp. 255–263.

[4] Aylor, J. H., Thieme, A., and Johnson, B. W., 1992. "A battery state-of-charge indicator for electric whelchairs". *IEEE Transactions on Industrial Electronics,* ***29***(5), October, pp. 398–409.

[5] Chen, P.-C., and Koh, Y.-F., 2012. "Residual traveling distance estimation of an electric wheelchair". In 2015 5th International Conference on BioMedical Engineering and Informatics (BMEI 2012), IEEE, pp. 790–794.
[6] Bouquain, D., Blunier, B., and Miraoui, A., 2008. "A hybrid fuel cell/battery wheelchair - modeling, simulation and experimentation". In Vehicle Power and Propulsion Conference, IEEE.
[7] Yang, Y.-P., Guan, R.-M., and Huang, Y.-M., 2012. "Hybrid fuel cell powertrain for a powered wheelchair driven by rim motors". *Journal of Power Sources*, pp. 192–204.
[8] Nice, K., 2001. *How Fuel Gauges Work*, apr. http://auto.howstuffworks.com/fuel-gauge.htm.
[9] Codeca, F., Savaresi, S. M., and Rizzoni, G., 2008. "On battery state of charge estimation: a new mixed algorithm". In 17th IEEE International Conference on Control Applications, Part of 2008 IEEE Multi-conference on Systems and Control, IEEE.
[10] Plett, G. L., 2004. "Extended kalman filtering for battery management systems of lipb-based hev battery packs part 2. modeling and identification". *Journal of Power Sources,* ***134***(2), aug, pp. 262–276.
[11] Plett, G. L., 2015. *Battery Management Systems*, first ed., Vol. 1. Artech House, 685 Canton Street.
[12] Coleman, M., Lee, C. K., Zhu, C., and Hurley, W. G., 2007. "State-of-charge determination from emf voltage estimation: Using impedance, terminal voltage, and current for lead-acid and lithium-ion batteries". *IEEE Transactions on Industrial Electronics,* ***54***(5), oct, pp. 2550–2557.
[13] Weng, C., Sun, J., and Peng, H., 2014. "A unified open-circuit-voltage model of lithium-ion batteries for state-of-charge estimation and state-of-health monitoring". *Journal of Power Sources,* ***258***, jul, pp. 228–237.
[14] Ng, K.-S., Huang, Y.-F., Moo, C.-S., and Hsieh, Y.-C., 2009. "An enhanced coulomb counting method for estimating state-of-charge and state-of-health of lead-acid batteries". In The 31th International Telecommunications Energy Conference, Vol. 31, IEEE.
[15] Simon, D., 2006. *Optimal State Estimation: Kalman, H Infinity, and Nonlinear Approaches*, first ed. Wiley-Interscience, jun.
[16] Plet, G. L., 2004. "Extended kalman filtering for battery management systems of lipb-based hev battery packs: Part 3. state and parameter estimation". *Journal of Power Sources,* ***134***(2), aug, p. 277292.
[17] Idaho National Laboratory, B. E. A., 2008. Battery test manual for plug-in hybrid electric vehicles revision. Tech. Rep. 0, US Department of Energy: Vehicle Technologies Program. Freedom Car Report.
[18] Coleman, M., Hurley, W. G., and Lee, C. K., 2008. "An improved battery characterization method using a two-pulse load test". *IEEE Transactions on Energy Conversion,* ***23***(2), jun, pp. 708–713.
[19] UPG, 2016. *UPG Sealed Lead-Acid Battery UB12350*. 1720 Hayden Drive, Carrollton, TX 75006.
[20] Miller, C. X., 2016. "A state-of-charge estimator for a semi-autonomous electric wheelchair". Undergraduate honors thesis, The Schreyer Honors College, The Pennsylvania State University.